Targeted Diet Modification Reduces Multiple Sclerosis-like Disease in Adult Marmoset Monkeys from an Outbred Colony

Kap, Yolanda S.; Bus-Spoor, Carien; van Driel, Nikki; Dubbelaar, Marissa L.; Grit, Corien; Kooistra, Susanne M.; Fagrouch, Zahra C.; Verschoor, Ernst J.; Bauer, Jan; Eggen, Bart J. L.

Published in:
Journal of Immunology

DOI:
10.4049/jimmunol.1800822

Publication date:
2018

The Journal of Immunology

Targeted Diet Modification Reduces Multiple Sclerosis –like Disease in Adult Marmoset Monkeys from an Outbred Colony

Yolanda S. Kap, Carien Bus-Spoor, Nikki van Driel, Marissa L. Dubbelaar, Corien Grit, Susanne M. Kooistra, Zahra C. Fagrouch, Ernst J. Verschoor, Jan Bauer, Bart J. L. Eggen, Hermie J. M. Harmsen, Jon D. Laman and Bert A. 't Hart

J Immunol published online 19 October 2018
http://www.jimmunol.org/content/early/2018/10/18/jimmunol.1800822

Supplementary Material **http://www.jimmunol.org/content/suppl/2018/10/18/jimmunol.1800822.DCSupplemental**

The Journal of Immunology is published twice each month by
The American Association of Immunologists, Inc.,
1451 Rockville Pike, Suite 650, Rockville, MD 20852

Print ISSN: 0022-1767 Online ISSN: 1550-6606.

Published October 19, 2018, doi:10.4049/jimmunol.1800822

Targeted Diet Modification Reduces Multiple Sclerosis–like Disease in Adult Marmoset Monkeys from an Outbred Colony

Yolanda S. Kap,* Carien Bus-Spoor,† Nikki van Driel,* Marissa L. Dubbelaar,‡ Corien Grit,‡ Susanne M. Kooistra,‡,§ Zahra C. Fagrouch,¶ Ernst J. Verschoor,¶ Jan Bauer,‖ Bart J. L. Eggen,‡,§ Hermie J. M. Harmsen,† Jon D. Laman,‡,§,1 and Bert A. 't Hart*,‡,§,1

Experimental autoimmune encephalomyelitis (EAE) in common marmosets is a translationally relevant model of the chronic neurologic disease multiple sclerosis. Following the introduction of a new dietary supplement in our purpose-bred marmoset colony, the percentage of marmosets in which clinically evident EAE could be induced by sensitization against recombinant human myelin oligodendrocyte glycoprotein in IFA decreased from 100 to 65%. The reduced EAE susceptibility after the dietary change coincided with reduced *Callitrichine herpesvirus 3* expression in the colony, an EBV-related γ1-herpesvirus associated with EAE. We then investigated, in a controlled study in marmoset twins, which disease-relevant parameters were affected by the dietary change. The selected twins had been raised on the new diet for at least 12 mo prior to the study. In twin siblings reverted to the original diet 8 wk prior to EAE induction, 100% disease prevalence (eight out of eight) was restored, whereas in siblings remaining on the new diet the EAE prevalence was 75% (six out of eight). Spinal cord demyelination, a classical hallmark of the disease, was significantly lower in new-diet monkeys than in monkeys reverted to the original diet. In new-diet monkeys, the proinflammatory T cell response to recombinant human myelin oligodendrocyte glycoprotein was significantly reduced, and RNA-sequencing revealed reduced apoptosis and enhanced myelination in the brain. Systematic typing of the marmoset gut microbiota using 16S rRNA sequencing demonstrated a unique, Bifidobacteria-dominated composition, which changed after disease induction. In conclusion, targeted dietary intervention exerts positive effects on EAE-related parameters in multiple compartments of the marmoset's gut-immune–CNS axis. ***The Journal of Immunology*****, 2018, 201: 000–000.**

Multiple sclerosis (MS) is a neurologic disease associated with dysregulated reactions by the adaptive arm of the immune system against CNS Ags (1). The trigger of MS is not known but is thought to involve dynamic interactions of genetic and environmental risk factors, infection with the γ1-herpesvirus EBV in particular (2–4). A factor that is suspected to underlie the current increasing prevalence of MS is an altered gut microbiota marked by reduction of beneficial bacteria and an increase of pathobionts (5). Indeed, MS patients have a different gut microbiota composition compared with healthy controls (6–10) that may affect T and B cell functions (9–11).

There is compelling evidence from a well-established MS animal model, experimental autoimmune encephalomyelitis (EAE), that gut microbiota exerts profound effects on disease expression in young adolescent (8–12 week) specific pathogen free (SPF)-bred mice (9, 10). However, it is unclear whether such effects can be translated to the more robust human immune system that has been trained by the lifelong exposure to environmental pathogens. This question has been addressed in a well-validated nonhuman primate model of MS, EAE in common marmosets (*Callithrix jacchus*).

Common marmosets are highly susceptible to EAE and provide translationally relevant EAE models that display clinical and pathological similarity with MS (12, 13). The susceptibility to EAE involves the presence of autoreactive effector memory T cells in the pathogen-trained immune repertoire. Evidence indicates that these autoreactive cells are induced by chronic

*Department of Immunobiology, Biomedical Primate Research Centre, 2280 GH Rijswijk, the Netherlands; †Department of Medical Microbiology, University Medical Center Groningen, University of Groningen, 9713 GZ Groningen, the Netherlands; ‡Section Medical Physiology, Department of Neuroscience, University Medical Center Groningen, University of Groningen, 9713 AV Groningen, the Netherlands; §MS Centrum Noord Nederland, 9722 NN Groningen, the Netherlands; ¶Department of Virology, Biomedical Primate Research Centre, 2288 GJ Rijswijk, the Netherlands; and ‖Department for Neuroimmunology, Center for Brain Research, Medical University of Vienna, A-1090 Vienna, Austria

[1]J.D.L. and B.A.t.H. share senior authorship.

ORCIDs: 0000-0003-0708-7981 (Y.S.K.); 0000-0002-4930-1467 (M.L.D.); 0000-0003-0211-8283 (S.M.K.); 0000-0001-8941-0353 (B.J.L.E.); 0000-0001-5085-9807 (J.D.L.); 0000-0002-0036-5267 (B.A.t.H.).

Received for publication June 12, 2018. Accepted for publication September 25, 2018.

Y.S.K., J.D.L., and B.A.t.H. have designed the study; Y.S.K. and N.v.D. performed the in vivo study; C.B.-S. performed the microbiota experiments; N.v.D. performed the ex vivo immunological analyses; M.L.D., S.M.K., C.G., and B.J.L.E. performed the RNA sequencing of the brain; J.B. performed the neuropathology; Z.C.F. and E.J.V. performed the *Callitrichine herpesvirus 3* analyses; H.J.M.H. supervised the microbiota analyses; Y.S.K., H.J.M.H., J.D.L., and B.A.t.H. wrote the paper.

Address correspondence and reprint requests to Dr. Yolanda S. Kap, Department of Immunobiology, Biomedical Primate Research Centre, Post Office Box 3306, 2280 GH Rijswijk, the Netherlands. E-mail address: kap@bprc.nl

The online version of this article contains supplemental material.

Abbreviations used in this article: CalHV3, *Callitrichine herpesvirus 3*; EAE, experimental autoimmune encephalomyelitis; FISH, fluorescent in situ hybridization; IPA, ingenuity pathway analysis; LLN, lumbar lymph node; MNC, mononuclear cell; MOG, myelin oligodendrocyte glycoprotein; MS, multiple sclerosis; PC, principal component; rhMOG, recombinant human MOG; SLO, secondary lymphoid organ; SPF, specific pathogen free; WBS, water-based supplement; WM, white matter; YBS, yogurt-based supplement.

infection with a CMV-related virus and are reactivated by B cells infected with the EBV-like virus *Callitrichine herpesvirus 3* (CalHV3), which is causally associated with the cause of EAE (14–16). The unique possibility to evoke EAE in marmosets with a relatively mild induction protocol lacking innate immune stimulation by bacterial Ags (recombinant human myelin Ag, myelin oligodendrocyte glycoprotein [MOG] [rhMOG] in the mineral oil IFA, a formulation ineffective in SPF mice) is based on the reactivation of these autoreactive effector memory T cells (12).

We report that after the introduction of a new dietary supplement in our conventionally-housed, purpose-bred marmoset colony, the frequency of monkeys in which EAE could be induced with rhMOG/IFA unexpectedly decreased from 100 to 65%. This reduced EAE susceptibility coincided with a sharp reduction of CalHV3 expression in blood. These findings prompted a controlled study to assess which EAE-related parameters were affected by the change from the old water-based supplement (WBS) to the new yogurt-based supplement (YBS). The study involved eight adult twins, which, because of their natural bone marrow chimerism, are immunologically strongly comparable. All animals had been raised on the YBS for at least 12 months prior to the inclusion in the study. Of each twin, one sibling was reverted to the WBS starting eight weeks before EAE induction, whereas the other sibling was maintained on the YBS. We observed that this short course of dietary intervention was sufficient to restore the impaired EAE prevalence from 75 to 100% as well as to revert the significantly reduced CNS pathology. We observed profound systemic effects of the dietary modification in multiple compartments along the gut-immune–CNS axis. These findings open new avenues for translational research into the effects of food and microbiota on autoimmune and neurologic diseases in a species that replicates the genetic, immunological, and microbial complexity of humans.

Materials and Methods

Animals

Data reported in this study were collected in marmosets from the purpose-bred colony of the Biomedical Primate Research Centre (Rijswijk, the Netherlands). For the targeted diet intervention experiment, eight adult dizygotic bone marrow–chimeric twin pairs of equal gender and adult age were randomly selected (Table I). All monkeys had been raised for at least 12 mo on the YBS, which was introduced in the colony in January 2014. From each twin pair, one randomly selected sibling was assigned to remain on the modified (new) diet, whereas the fraternal sibling was fed the original (classic) diet that was used before 2014. Before entry into the experiment, each monkey was health checked for clinical and microbiological abnormalities. Only monkeys declared healthy by the institute's veterinary staff were used. Fraternal twin siblings were stratified over both groups in such a way that body weights were not significantly different between both groups. Monkeys were pair-housed with monkeys of the same diet group (Table I) in spacious cages enriched with branches and toys and with padded shelter provided on the floor.

Diet

The experimental variable in this study is the composition of a dietary supplement, which was altered in January 2014. Marmosets kept in captivity have complex dietary needs, which are satisfied by providing a dietary supplement (porridge) on top of the commercial food pellets for New World monkeys (Special Diet Services, Witham, Essex, U.K.). Whereas food pellets and drinking water are provided ad libitum, the provision of supplements is more strictly regulated. In the situation before the dietary change in 2014, each marmoset was given 20 ml of a WBS four times a week (specified in Table II). In the situation after 2014, each marmoset was given 9 ml of a YBS (Table II) every day. Table II shows the diet constituents expressed as weekly dosage per marmoset and Table III details the vitamin intake via the supplement.

In addition to the food pellets and supplement, the WBS group received apples and oranges three times per week, whereas the YBS group received apple, orange, grape, pear, and broad beans every day. Moreover, the marmosets were given play-and-food-enrichment several times a week. In the WBS group, this consisted of mealworms, Arabic gum, and raisins, whereas in the YBS group this consisted of Arabic gum, peanuts, and bread.

Ethics

All experimental procedures had been reviewed and approved by the Institute's Animal Ethics Committee prior to the start of the study, and monkeys were housed and handled according to the Dutch Law on animal experimentation. The animal facilities of Biomedical Primate Research Centre are regularly inspected and accredited by the Association for Assessment and Accreditation of Laboratory Animal Care International in full.

EAE induction

EAE was induced with rhMOG, a recombinant protein encompassing the extracellular domain of human MOG residues 1–125, which was produced in *Escherichia coli* and purified as described previously (17). The inoculum contained 100 μg rhMOG in 200 μl PBS, which was emulsified in 200 μl IFA (Difco Laboratories, Detroit, MI) by gentle stirring for at least 1 h at 4°C. The emulsion was injected at four spots of 100 μl into the dorsal skin under sedation by alfaxalone (10 mg/kg alfaxan i.m.; Vetoquinol, Den Bosch, the Netherlands) and ketamine (10 mg/kg i.m.; AST Farma, Oudewater, the Netherlands), with booster immunizations given every 28 d until development of overt neurologic disease (EAE score $\geq$2) was observed. Marmosets were monitored and signs of EAE were scored on a daily basis using a standard scoring system (18). Overt neurologic defects are represented by the following score: 2 = ataxia or optic disease; 2.5 = paresis of two limbs. Animals with EAE score $<$2 are indicated asymptomatic.

After immunization at day 0, one animal developed score 2 before day 28 and was not given a booster immunization (M14002), whereas eight marmosets needed one boost (M13004, M13005, M14006, M14009, M14014, M14015, M14025, and M14031) and five marmosets needed two boosts (M13046, M14005, M14010, M14024, and M14032). Two marmosets (M13047 and M14001) were boosted three times, but they did not develop clinical symptoms within the predetermined time frame of the experiment. These two monkeys were indicated as non-EAE in text and figures.

According to the ethics requirements, a monkey was euthanized within 3 d after development of EAE score 2.5 (paresis of one or more limbs) or at the predetermined end (120 d after immunization) when they did not reach this EAE score.

Blood and tissue collection

For cellular and humoral immune profiling during the course of the study, venous blood samples ($<$1.5 ml) were collected from the femoral vein an put into EDTA Vacutainers (Greiner Bio-One, Alphen aan den Rijn, the Netherlands). Plasma and mononuclear cells (MNC) were isolated as described below.

Marmosets reaching the EAE score 2.5 were deeply sedated by i.m. injection of alfaxalone for collection of the total venous blood volume and were subsequently euthanized by infusion of sodium pentobarbital (euthesate; Apharmo, Duiven, the Netherlands). Upon necropsy, lymph nodes from axillary, inguinal, lumbar (LLN), mesenteric, and cervical regions, as well as the spleen, were harvested. The brain, spinal cord, and optic nerve were collected for histology (formalin) and immunohistochemistry or RNA sequencing (snap-frozen in liquid nitrogen).

MNC from blood (PBMC) and from secondary lymphoid organs (SLO) were isolated as previously described (18). Hematology and serum chemistry were measured on a Sysmex XT-2000i analyzer and a COBAS Integra 400 plus, respectively.

PCR for CalHV3

CalHV3 levels were determined with a diagnostic PCR, detecting only the presence or absence of the virus, and a quantitative PCR, which determines viral DNA copy numbers per microgram of total DNA. DNA was isolated from MNC or tissue using the QIAamp DNA Mini Kit (QIAGEN Benelux BV, Venlo, the Netherlands). For diagnostic purposes, a CalHV3-specific PCR was used, and the PCR fragments were analyzed by electrophoresis on a 1% agarose gel as described previously (19). For the quantitative PCR, DNA polymerase gene-specific primers and probe were designed based on the published sequence of CalHV3 (GenBank accession number NC004367; https://www.ncbi.nlm.nih.gov/nuccore/NC_004367), and the assay was performed as described previously (19).

RNA sequencing of whole-brain tissue

Snap-frozen brain tissue from the middle region (including corpus callosum) was sectioned on a cryostat and collected in QIAzol Lysis Reagent (QIAGEN

Benelux BV), followed by RNA extraction using an RNeasy Lipid Tissue Mini Kit (QIAGEN Benelux BV), according to manufacturer's protocol. RNA quality was determined using a Fragment Analyzer Automated CE System in combination with the Standard Sensitivity RNA Analysis Kit (Advanced Analytical Technologies, Ankeny, IA). Using a Quantseq 3′mRNA-Seq Library Prep Kit (Lexogen GmbH, Vienna, Austria), according to manufacturer's protocol (version after February 2017), sequencing libraries were generated, starting from 500 ng RNA with an average RNA integrity number of 8.9 (±0.4). cDNA fragment libraries were sequenced on an Illumina HiSeq 2500 using default parameters (single read 1 × 50 bp) in pools of multiple samples.

Sequencing reads were aligned against the Callithrix jacchus (Ensembl v82) genome with the use of Hisat v0.1.5 (20), allowing a maximum of two mismatches. Aligned reads were subsequently sorted with SAMtools v.1.2 (21). HTSeq v0.6.1 (22) was used for gene level quantification with the default parameters, except when "mode = union" and "stranded = no." A quality control check was performed on the generated FASTQ files with the use of FastQC v.0.11.3 (http://www.bioinformatics.babraham.ac.uk/projects/fastqc), Picard v1.130 (http://broadinstitute.github.io/picard), and SAMtools.

With the use of the data-adaptive flag method for RNA-sequencing (23), genes with low expression levels were filtered. Genes were included in the downstream analysis when observed above the threshold calculated with the data-adaptive flag method for RNA-sequencing in at least half of the samples. A correction for the twin-set batch was made on the count per million values with the function "removeBatchEffect" of the limma package to extract the diet effects. Differential gene expression was determined by comparing WBS and YBS. Genes were considered differentially expressed when a LogFC >1 or LogFC < −1 and a p value <0.01 was observed. For visualization, Pearson correlation–based clustering analysis (function hclust, method equals "complete") was performed to distinguish subsets of genes showing similar transcriptional regulation.

Microbiota analysis of fecal samples

Fecal samples of individual marmosets were collected at several time points during the study when the marmosets were separated for a few hours to recover from sedation. Fecal samples of all monkeys were collected at the following time points: before the diet change (day −56), 7 wk after the diet change (i.e., 1 wk before EAE induction [day −7]), and 3 wk (day 21) or 7 wk (day 49) after EAE induction. From the two marmosets that remained without clinical symptoms, fecal samples were additionally collected at day 77 and 105 post-EAE induction. Fecal samples were stored at −80°C until analysis (24, 25). Total DNA was extracted by use of the double bead-beating method described by Yu and Morrison (26) with some modifications. Mechanical cell disruption was performed with four glass beads (4 mm) and 0.5-g zirconium beads (0.1 mm) per sample at 5.5 ms^{-1}, 3 cycles of 1 min with 30 s intervals using a Precellys 24 (Bertin Technologies, Montigny-le-Bretonneux, France). Subsequently, the samples were heated at 95°C. The protein precipitation with 10 M ammonium acetate was performed twice. Purity was measured by NanoDrop 2000 (Thermo Fisher Scientific, Wilmington, DE).

The extracted DNA was amplified and processed as previously described (27). Briefly, primers covering the V3 and V4 hyper V region of the bacterial 16S rRNA genes were used. The 341F and 806R primers with a 6-nt barcode were described previously (28). Presence of a product was confirmed by agarose gel. The length per read was around 465 bases per bacteria. Samples were cleaned by using Agencourt AMPure XP magnetic beads (Beckman Coulter, Pasadena, CA). DNA concentrations were measured using a Qubit 2.0 Fluorimeter, and library normalization was performed to have an equal amount of sample representation in the final pool. Sequencing was performed on an Illumina MiSeq using a PhiX library as a control.

Data analysis of the sequenced samples included PANDAseq QIIME pipelines, and sample composition was identified to species level by ARB software (29–31). A principal component (PC) analysis was used to describe the variation in the bacterial composition of the samples. In this study, PC1 described 79% of the variation in data. The Simpson diversity index was used to determine microbial diversity.

The presence of Bifidobacteria was analyzed by fluorescent in situ hybridization (FISH) as described previously (25). Briefly, a feces sample (0.25 g) of a YBS-fed marmoset on day −56 was diluted 10× in PBS and fixed with 4% paraformaldehyde. The fixed sample (10 μl) was applied to gelatin-coated glass slides and dehydrated with 96% ethanol. Slides were hybridized at 50°C overnight in hybridization buffer containing 5 ng/μl fluorescently labeled probes. Bacterial density in the sample was characterized by hybridization with a FITC-labeled universal bacterial 16S rRNA–targeted, fluorescein-labeled oligonucleotide probe EUB338, and Bifidobacteria were visualized with a CY3-labeled Bif164 probe (both probes were obtained from Eurogentec, Seraing, Belgium). Slides were washed at 50°C in hybridization buffer without SDS and mounted with VECTASHIELD (Vector Laboratories, Burlingame, CA). Slides were examined using the Leica fluorescence microscope (Leica Microsystems, Wetzlar, Germany). Raw images of the slides were merged and optimized using Adobe Photoshop software. Bifidobacterial cells are ∼3–5 μm in length and 1 μm in width.

Ab levels in immune plasma

Plasma samples were prepared from whole blood and stored in aliquots at −20°C. Ab binding to nonglycosylated rhMOG and MOG peptides (24–46, 34–56, 54–76) was analyzed by ELISA as described previously (18). ELISA data were normalized against a standard curve of a plasma pool (made with necropsy plasma of three EAE marmosets from a previous study). The Ab content in the pooled plasma was defined at 2.500 arbitrary units, and newly collected ELISA data were fitted to a four-parameter hyperbolic function using the homemade ADAMSEL program developed by Dr. E. Remarque (Biomedical Primate Research Centre, the Netherlands).

T cell proliferation and cytokine production

MNC isolated from peripheral blood or SLO were tested for proliferation against the Ags MOG34–56 (5 μg/ml) and rhMOG (5 μg/ml) and the mitogen Con A (5 μg/ml) as described previously (18). Incorporation of [^{3}H]thymidine (0.5 μCi/well) was determined using a Matrix 9600 β-counter (Packard 9600; Packard Instrument, Meriden, CT). Results are expressed as a stimulation index, which is calculated by dividing the average cpm of stimulated cells by the average cpm of unstimulated cells. A stimulation index above 2 is set as cutoff for a positive proliferative response as customary for primate T cell responses.

Cytokine levels were measured in supernatant of cell cultures that were stimulated for 48 h with rhMOG or MOG34–56. ELISAs detecting IL-17A and IFN-γ were performed according to instructions of the manufacturer (U-CyTech, Utrecht, the Netherlands).

Cellular phenotyping

PBMC and MNC from SLO were phenotyped by flow cytometry (18). Briefly, cells were stained with the Fixable Viability Dye eFluor 506 (eBioscience, San Diego, CA) to exclude dead cells. For phenotyping, cells were stained with commercially available mAbs against CD3 (SP43-2), CD4 (L200), CD27 (MT721), CD45RA (5H9), CD56 (NCAM 16.2), and HLA-DR (L243) (all from BD Biosciences, San Diego, CA); mAbs against CD20 (H299; Beckman Coulter), CD40 (B-B20; Abcam, Cambridge, U.K.), and CD8 (LT-8; AbD Serotec, Dusseldorf, Germany) were also used. After staining, cells were fixed in 1% BD Cytofix (BD Biosciences). Flow cytometric measurements were performed using the BD FACSAria LSR II, and data were analyzed with FlowJo software (Treestar, Ashland, OR). The gating strategy to determine phenotype was as follows: Live cells were first selected as viability dye negative cells. Next, single lymphocytes were identified based on forward scatter and side scatter. Within the live lymphocyte population, $CD3^-$ and $CD3^+$ cells were determined. Within the $CD3^+$ T cell population, $CD4^+CD8^-$ and $CD4^-CD8^+$ cells were distinguished. The figures show the percentage of cells within the parent gate, which is indicated before the forward slash (/).

Immunohistochemistry and histology

Immunohistochemical staining was performed on paraffin-embedded tissue obtained at necropsy. Paraffin sections were cut into 3–5 μm, deparaffinized, and stained with H&E and Luxol fast blue/periodic acid–Schiff to assess inflammation and demyelination. Inflammation was visualized by staining infiltrating cells with H&E. The inflammatory index of the spinal cord is given as the average number of inflamed blood vessels per spinal cord cross section (10–12 sections per animal). Demyelination in the spinal cord was measured on a total of 10–12 cross sections by using a morphometric grid. Demyelination in the brain was determined as follows: Brain sections stained for Luxol fast blue/periodic acid–Schiff were scanned at 1000 dpi with an Agfa DuoScan scanning device. Images were then imported into the public domain program ImageJ (version 1.46r). In density slice mode, first the total amount of white matter (WM) was measured. Lesions in the WM were selected by freehand mode, and their size was measured. Finally, demyelination in WM was calculated as percentage of total WM. Six sections of the brain of each animal were analyzed, amounting to ∼6 cm^2 of WM in total.

Statistics: power analysis

Historical data showed that the change from the old WBS to the new YBS was associated with a reduction of EAE prevalence from 100 to 65%

(see Fig. 1A). Using this clinical-effect estimator, we performed a power analysis for the group size in the twin study, indicating that 19 monkeys per group would be required for 80% power (with α set at 0.05). To avoid such excessive animal numbers for an explorative study, we chose to include eight twins, which, because of the bone marrow chimerism, are immunologically highly comparable.

Clinical data are presented as disease-free survival curves using the Kaplan–Meier estimator. Difference in disease-free survival was statistically tested using the log-rank test. Individual data are presented as dot plots, with bars indicating median values. statistical analysis was performed using Prism 7.0c for Mac OS X. Between-group comparisons were made using the Wilcoxon signed-ranked test. A p value < 0.05 was considered statistically significant.

Because microbial abundances are rarely distributed normally, nonparametric tests were used. Changes in the composition at different time points were analyzed with a Friedman test followed by a post hoc sign test to compare medians. A Mann–Whitney U test was used to compare medians of two groups and the Spearman test was used for correlation within the microbiota data. All tests were two-tailed, and a p value < 0.05 was considered significant. All statistical analyses were performed using IBM SPSS Statistics 24.0.

Results

Dietary modification reduces clinical EAE symptoms and CalHV3 levels

Marmosets living in captive colonies are at risk to develop clinical conditions associated with nutritional deficiencies, such as idiopathic marmoset wasting syndrome (32) or severe osteomalacia (33). Hence, optimization of their diet is a continuous concern. In their natural habitat, marmosets have a varied diet that includes fruits, insects, and especially the plant exudates gum, sap, latex, and resin. To accommodate the high dietary needs of marmosets held in captivity, they are given dietary supplements in addition to the standard food pellets. In 2014, the composition of the dietary supplement given to our pedigreed marmoset colony (Table I) was changed. The modification comprised doubling of the amount of vitamin B and fiber content and usage of yogurt instead of water as the basis (contents of the supplements are specified in Tables II, III). We observed that after this dietary modification, the prevalence of rhMOG/IFA–induced EAE in the colony decreased from 100 to 65%, although the time to disease onset was significantly prolonged (Fig. 1A). These observations suggest, but do not prove, a causal relation between the modification of the dietary supplement and the reduced susceptibility to EAE.

To assess aspects of the EAE model affected by the diet change, we set up a controlled study in marmoset twins (Table I). Marked differences in general health parameters, such as bodyweight or hematology/serum chemistry values, between both groups were not found (Table I and Supplemental Fig. 1). All twin siblings that were reverted to the WBS at 8 wk preimmunization developed clinically evident EAE. Two of the eight (25%) fraternal siblings given YBS failed to develop clinically evident EAE, and three of the eight YBS monkeys developed clinical EAE later than their fraternal sibling receiving the WBS (Fig. 1B, 1C). Note that the reduced EAE prevalence of 75% (Fig. 1B) was in the range of the historical data obtained in the colony (Fig. 1A). These data indicate that the reduced EAE susceptibility of 75% could be reverted to the original 100% by a relatively short course on the original WBS. Although the difference in survival between the two groups was not significant, the data (Fig. 1B) fitted perfectly with data from the historical studies (Fig. 1A). This increased the number of monkeys and revealed that the delay in clinical EAE symptoms in YBS monkeys is even more significant than for the historical studies alone (Fig. 1D).

Another observation associated with the diet change was the reduced expression of CalHV3, a marmoset B cell–transforming γ1-herpesvirus closely related to EBV, in peripheral blood of marmosets in our colony (Fig. 1E). Marmosets are naturally infected with CalHV3, and CalHV3-infected B cells have a crucial pathogenic role in the marmoset EAE model (15, 34–36). CalHV3 DNA levels were also analyzed in blood and SLO collected in the twin study. In one animal (M14005, WBS), CalHV3 could not be detected. In monkeys M13047 and M14001 (both YBS), the monkeys without clinical EAE symptoms, CalHV3 was only detected in the LLN, but levels were too low for quantification. Quantitative PCR revealed that CalHV3 copy numbers were lower in the YBS group compared with the WBS group (Fig. 1F).

The new diet reduces demyelination and alters brain gene expression

To determine whether the dietary modification affected the CNS, spinal cord demyelination was quantified by histology. Moreover, gene expression profiles of the EAE-affected brain were studied. Although six of the eight monkeys in the YBS group reached clinical score 2.5, significantly less demyelination was observed in the spinal cord of YBS monkeys (25.6 ± 15.4%) than in WBS monkeys (41.3 ± 7.4%; Fig. 2, Table I). Demyelination was observed in the brain of five monkeys from the WBS group and in three from the YBS group (Table I).

To obtain additional data on the effect of the dietary modification on the brain, we performed a pairwise comparison of transcriptome patterns of the middle brain, which includes predilection areas of WM lesions, of WBS and YBS monkeys, resulting in 295 differentially expressed genes (p value <0.01, LogFC >1; Fig. 3A, Supplemental Table I). Two hundred and twenty-nine genes (208 annotated) were more abundantly expressed in YBS monkeys and sixty-six genes (48 annotated) were more abundantly expressed in WBS brain. Ingenuity pathway analysis (IPA) revealed that WBS and YBS were associated with different pathways (Fig. 3B, 3C). The CNS of YBS monkeys showed higher expression of genes related to integrin, phospholipase C, and CXCR4 signaling, which are all related to oligodendrocyte functioning and myelination (PMID 21637375, PMID 29142295, PMID 19570026, and PMID 20534485). Among the genes that were more abundantly expressed in the YBS monkeys, those related to apoptosis were overrepresented. The majority of these genes are involved in suppressing apoptosis, suggesting that feeding the YBS resulted in reduced apoptosis in the CNS (Supplemental Table I). We finally used the Molecular Signatures Database (PMID 16199517) and data mining in Pubmed to identify genes involved in myelin structure, biogenesis, maintenance, and repair. This myelin gene set was overlaid with the list of differentially expressed genes, yielding several myelin-related genes that were differentially expressed between WBS- and YBS-fed monkeys. Interestingly, all these genes were more abundantly expressed in the brains of monkeys fed the YBS (Fig. 3D). In summary, RNA-sequencing analysis of CNS tissue provided evidence for lower apoptosis and higher myelination in monkeys fed the YBS compared with those fed the WBS.

Diet modification alters immune responses

We speculated that the reduced EAE prevalence and pathology in the YBS-fed monkeys is associated with an altered immune response. To assess this, autoantibody levels and T cell reactivity were determined. In both groups, including the two non-EAE monkeys, similar plasma levels of IgG against rhMOG and MOG peptides were detected, excluding a relevant influence of the dietary modification on this parameter (Supplemental Fig. 2A, 2B). Cellular responses against rhMOG and MOG peptides were assayed by ex vivo restimulation of MNC isolated from blood and SLO. In the YBS-fed group, significantly less rhMOG-induced

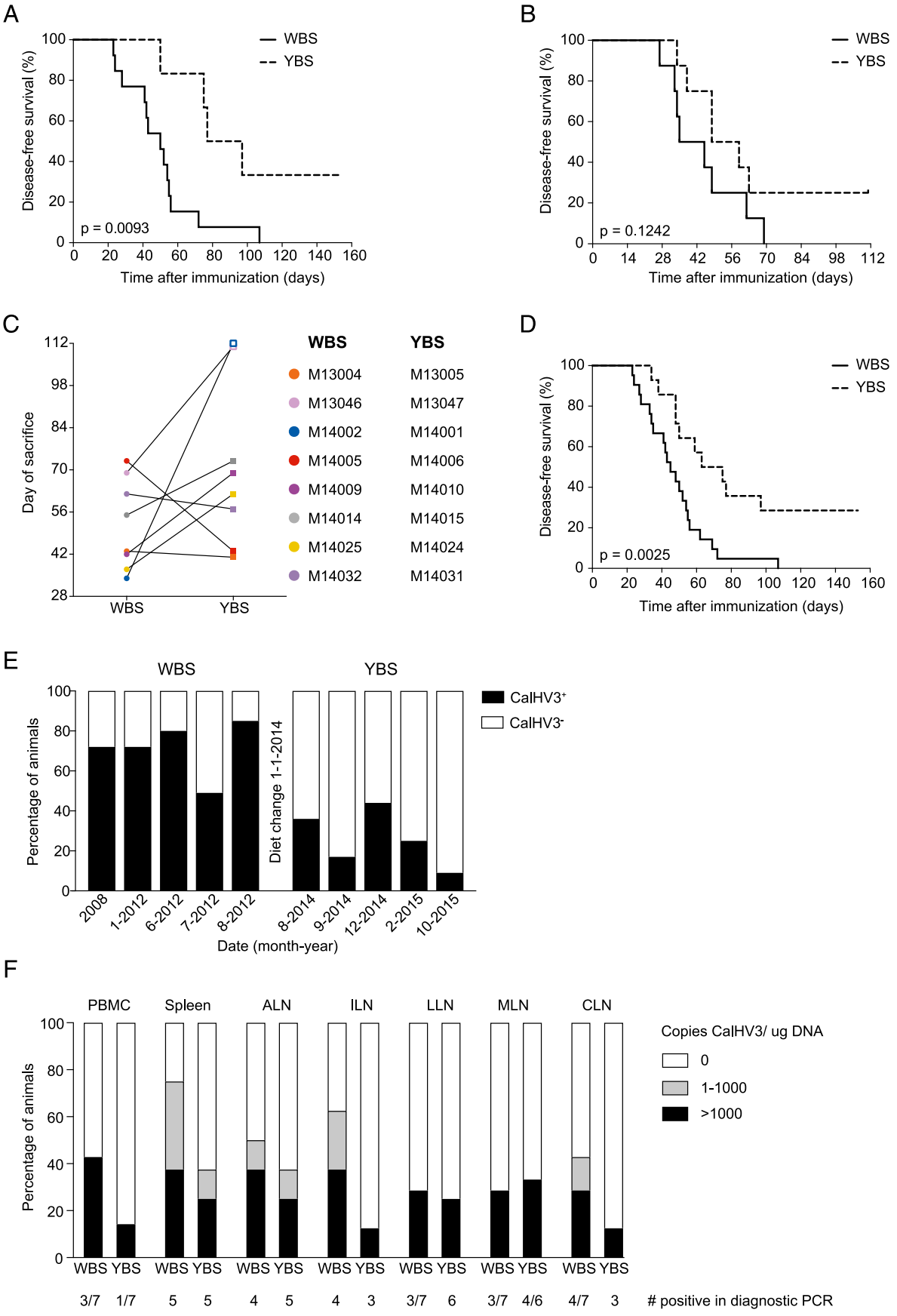

FIGURE 1. Dietary modification affects EAE susceptibility, spinal cord demyelination, and CalHV3. (**A**) Time to clinical score 2 (log-rank test) of historical studies before (n = 13 marmosets, WBS) and after (n = 6 marmosets) the introduction of YBS. (**B**) Survival graph of twin study. Shown is time to clinical score 2 (log-rank test). (**C**) Paired analysis of the day of sacrifice. Asymptomatic monkeys are indicated by an open square. (**D**) Time to clinical score 2 obtained in the twin study was combined with the historical data depicted in (A). Monkeys of the WBS (n = 21) develop *(Figure legend continues)*

Table I. Animal features, clinical data, and pathology scores

	Animal features				Clinical[a]			Pathology			
								Demyelination (%)			Inflam. Index
	Gender	Weight[b]	Age[c]	Cage[d]	PSD Score 2	DOS	Body Weight Loss (%)	Optic Nerve	Brain WM[e]	Spinal Cord[f]	Spinal Cord[g]
WBS											
M13004[h]	F	388	41	11	35	43	5.4	21	0.2	42.8	2.5
M13046[h]	M	374	33	2	62	69	4.8	84	4.8	48.9	2.5
M14002	M	371	29	2	27	34	11.1	0	0	36.3	2.5
M14005	M	435	27	3	69	73	13.1	0	0.9	56.6	2.5
M14009	F	338	27	10	34	42	4.7	0	0	34.9	2.5
M14014	F	365	26	7	45	55	4.1	93	2.4	40.3	2.5
M14025	M	345	24	3	33	37	6.9	0	0	32.9	2.5
M14032	F	457	22	7	48-49, 59	62	17.9	100[i]	1.5	37.8	2.5
YBS											
M13005[h]	F	478	41	6	34	41	7.1	29	5.3	26.8	2.5
M13047[h]	M	393	33	1	—	111	13.5	93	0	17.3	0.5
M14001	M	338	29	5	—	111	6.8	0	0.6	1.1	0.5
M14006	M	427	27	4	38	43	12.4	0	0	45	2.5
M14010	F	368	27	6	63	69	11.7	2	0	8.2	2.5
M14015	F	453	26	8	48	73	16.1	75	0	31	2.5
M14024	M	380	24	4	59	62	7.9	0	0	26.9	2.5
M14031	F	452	22	9	48	57	21.7	0	0.8	48.1	2.5

[a]All animals were sacrificed with score 2.5, except M13047 and M14001, which were sacrificed with score 0.5. Bodyweight loss at necropsy is shown as percentage of start weight.
[b]Weight in grams.
[c]Age in mo at day of immunization.
[d]Some monkeys were single-housed or housed with another monkey not involved in this experiment.
[e]Demyelination in the WM of the brain was determined in six brain sections per animal (~6 cm^2 of WM in total).
[f]Demyelination in the spinal cord was measured in a total of 10–12 cross sections by using a morphometric grid.
[g]The average number of inflamed blood vessels per spinal cord cross section (10–12 sections per animal). M14032 had optic neuritis at post sensitization day (PSD) 48–49.
[h]These monkeys were born under the WBS but were raised from 10 mo (M13004/13005) and 3 mo of age (M13046/M13047) on the YBS until start of the current experiment.
[i]M14032 had optic neuritis at PSD 48–49.
DOS, day of sacrifice; Inflam., inflammatory; PSD post sensitization day.

proliferation was detected in the axillary lymph nodes and inguinal lymph nodes, which drain the Ag/IFA inoculation sites, as well as in the mesenteric lymph nodes that drain the gut (Fig. 4). Not only proliferative responses were reduced in the YBS-fed group, but also the rhMOG-induced production of IL-17A and IFN-γ, two critical proinflammatory cytokines in EAE, was reduced in these lymph nodes (Fig. 4). No differences between groups were observed for the anti-inflammatory cytokines IL-4, IL-10, and TGF-β (data not shown).

We also examined whether the dietary change had altered the distribution of T and B cells in blood and SLO. Although no consistent effect of the dietary modification was observed on the distribution of the different T cell and B cell subsets assayed by flow cytometry (Supplemental Fig. 2C), there were some noticeable changes: 1) Significantly lower percentages of $CD45RA^-$ cells were observed in $CD8^+$ T cells isolated from the spleen and in the $CD4^+$ T cell population of the spinal cord–draining LLN of YBS-fed monkeys, indicative of a lower level of memory T cells involved in disease induction (Fig. 5A, 5B). 2) The $CD8^+$ T cell subset lacking CD45RA and expressing CD56 was significantly reduced in the YBS-fed group compared with the WBS-fed fraternal siblings (Fig. 5C). A central pathogenic role for these memory $CD8^+$ T cells expressing the NK marker CD56 in marmoset EAE was demonstrated in previous studies (37, 38). 3) The percentage of CD27-expressing $CD3^-$ lymphocytes was reduced in the LLN of the YBS-fed monkeys. Although the cells could not be costained with the anti-CD20 mAb because of spectral overlap of fluorochromes, this suggests a reduced percentage of memory B cells (Fig. 5D). 4) Within the brain-draining cervical lymph nodes from monkeys fed the YBS, we observed a significantly lower percentage of activated B cells, characterized by CD20, CD40, and MHC class II expression (Fig. 5E). In none of the analyses could a distinction could be made between EAE and non-EAE monkeys of the YBS-fed group, except for the percentage of activated B cells in peripheral blood. The percentages of activated B cells in PBMC were markedly higher in both non-EAE monkeys compared with the EAE monkeys (Fig. 5F). The observation that these B cells are increased in the blood indicates that they may not have been recruited into the CNS to participate in the induction of EAE pathology.

In summary, feeding the YBS diet lowered cellular autoimmune responses implicated in the EAE model, which was reflected by reduced Ag-stimulated proliferation and proinflammatory cytokine production and the numbers of memory B and T cells.

Gut microbiota changes following diet and immunization

We anticipated that the effect of food on disease expression involves modification of the gut microbiota. To our knowledge, no literature data are available documenting the complete composition of marmoset gut microbiota. To address this issue, we collected

EAE significantly earlier than YBS monkeys ($n = 14$). (**E**) The percentage of monkeys in which CalHV3 was detected in whole blood by diagnostic PCR. (**F**) Quantitative levels of CalHV3 were divided into three ranges (i.e., no CalHV3, 1–1000 copies, and more than 1000 copies CalHV3 per μg DNA). Shown on the *y*-axis is the percentage of monkeys in these CalHV3 ranges. The number of monkeys positive for CalHV3 in the diagnostic PCR is shown below the graph.

Table II. Composition of the supplement

	Unit	WBS	YBS
Water	ml	52	0
Yogurt (pasteurized)	ml	6	37.8
Lemon juice	ml	1.4	2.5
Carrot juice	ml	1.4	2.5
Wheat germ oil	ml	0.4	0.73
Vitamin D	IU	48	84
Oatmeal	g	1	1.67
Yeast flakes	g	0.7	1.3
Honey	Tablespoons	0.2	0.3
Protifar	g	1.44	2.52
Vitamin powder[a]	g	0.72	1.26
Ground powder[b]	g	24.8	8.8
Banana	Number	0	0.14

This table shows the dose of constituents per marmoset per week.
[a]Vitamin powder from Orthica (Almere, the Netherlands).
[b]Ground powder V3840-000 for marmosets/New World monkeys, from Sniff Spezialdiäten GmbH Soest, the Netherlands.

fecal samples of all monkeys at the following time points: before the diet change (day −56), 7 wk after diet change and 1 wk before EAE induction (day −7), and 3 (day 21) or 7 wk (day 49) after EAE induction. From the two marmosets that remained free of clinical symptoms, fecal samples were additionally collected at day 77 and 105 post-EAE induction. The microbiota contents of the fecal samples were analyzed via V3-V4 amplicon sequencing of 16S rRNA.

In the fecal samples collected before EAE induction (day −56 and −7), Actinobacteria were the most abundant phylum, with 65.5% (±15.9%) of total reads, followed by Firmicutes (20.3 ± 6.0%), and Bacteroidetes (10.9 ± 7.5%) (Fig. 6A). Actinobacteria were mainly represented by Bifidobacteria and *Collinsella*, whereas the Firmicutes were especially represented by the Lachnospiraceae family (11.3 ± 6.1%), and the Bacteroidetes were represented by *Bacteroides* (5.4 ± 6.2%) and *Prevotella* (4.7 ± 3.0%) (Fig. 5C). Bifidobacteria was the largest family detected, containing the species *Bifidobacterium callitrichos* (31.2 ± 11.5%), *Bifidobacterium aersculapii* (11.2 ± 7.6%), *Bifidobacterium simiae* (3.6 ± 2.6%), and *Bifidobacterium stellenboschense* (2.6 ± 3.34%) (Fig. 6B). The relatively high percentage of Bifidobacteria could be confirmed by FISH (Supplemental Fig. 3A).

Next, we analyzed whether diet-related changes in microbiota associated with disease progression could be detected. Remarkably, twin siblings fed a different supplement for 7 wk nevertheless displayed an essentially unaltered microbiota composition before EAE induction (compare samples day −56 and −7) with two exceptions, namely a 2-fold increase of *Collinsella tanakaei* (sign test, $p = 0.031$) in the YBS group and a 3-fold decrease of *Marvinbryantia formatexigens* (sign test, $p = 0.016$) in the WBS group. Divergence of the fecal microbiota composition between both groups was first detectable at 3 wk after immunization. At the phyla level, the percentage of Actinobacteria declined to 56% (± 12.8) at day 21 and to 38% (±5.6) at day 49 for the WBS-fed animals, whereas the percentage of Firmicutes and Bacteroidetes increased to 33% (±5.7) and 26% (±9.3), respectively, at day 49 (Fig. 7A, Supplemental Fig. 3B). At the bacterial species level, we observed that *Bifidobacterium stellenboschense* showed an increase in the WBS group (sign test, $p = 0.016$) and in the YBS group (sign test, $p = 0.031$) at day 21 (Fig. 7A–C, Supplemental Fig. 3C, 3D). The degree of diversity reflected by the Simpson diversity index (Fig. 7D) was only slightly altered. Seven weeks after the immunization (day 49), being 15 wk after the diet change, a clear distinction was observed between the two groups (Fig. 7C, 7E, Supplemental Fig. 3C, 3D), with lower abundance in the WBS group compared with YBS of *Bifidobacterium callitrichos, Bifidobacterium stellenboschense*, and *Bifidobacterium reuteri* and higher abundance of *Collinsella tanakaei* (Mann–Whitney *U* test, $p = 0.01$, 0.02, 0.01 and 0.01, respectively). This resulted in a higher percentage of *M. formatexigens*, *Bacteroides barnesiae*, and *Blautia stercoris* and a significantly lower number of total Bifidobacteria ($p = 0.01$) in the WBS group (Fig. 7A–C, Supplemental Fig. 3D).

Finally, we analyzed whether the two monkeys in the YBS group without clinical symptoms of EAE differed in gut microbiota composition from the symptomatic EAE monkeys in the same group. Until day 49, these two monkeys did not differ from the other monkeys in the YBS-fed group. After this time point, their fecal samples showed a reduction of PC1 and an increase of PC2 over time, corresponding to a reduction of *Bifidobacterium callitrichos* and an increase in *P. buccae*, *Bacteroides barnesiae*, and *M. formatexigens* (Fig. 7C, 7F, Supplemental Fig. 3).

In summary, in the first weeks after the diet change, no major changes in gut microbiota composition could be detected. Changes in the microbiota of the WBS-fed monkeys were detectable after activation of innate and adaptive immune responses by the immunization. This suggests a close interplay between diet, microbiota, and the immune system.

Table III. Vitamin intake via supplement

Vitamin	Chemical Name	Unit	WBS	YBS
A	Retinol	IU	719	636
B1	Thiamine	Mg	0.54	0.95
B2	Riboflavin	Mg	0.54	0.95
B3	Niacin/Niacinamide	Mg	6.3	11.0
B5	Pantothenic acid	Mg	1.8	3.2
B6	Pyridoxine	Mg	0.7	1.3
B11	Folic acid	Mg	27	47
B12	Cobalamin	Mg	0.92	1.72
C	Ascorbic acid	Mg	108	89
D3	Cholecalciferol	IU	194	237
E	Tocopherol	IU	12.6	16

This table shows the vitamin intake per marmoset per week.

Discussion

The risk to develop MS is determined by complex interactions of genetic (HLA in conjunction with around 200 SNP in other loci) and environmental risk factors, including infections as well as lifestyle factors (6–8, 39, 40). Mounting evidence from studies in animal models indicates a central role for the gut-immune–brain axis, but the exact influences of this axis on MS are unclear (41, 42). The dynamic interaction of genetic and environmental MS risk factors can be well modeled in a nonhuman primate, which, similar to humans, have a mature immune system that has been shaped by genetic diversity and the daily exposure to microbiota present within the body and in the environment. We previously reported that the pathogen-trained immune system of adult marmoset monkeys contains autoreactive T and B cells, which respond promptly to the inoculation of rhMOG/IFA (43), a formulation that is inactive in SPF-bred mice. The ensuing marmoset EAE model is characterized by neurologic deficits and CNS pathology reminiscent of relapsing-remitting MS. The impetus for the current study was the serendipitous observation that after the introduction of a modified dietary supplement, the percentage of marmosets in a random selection from an outbred colony that developed clinically evident EAE upon immunization with rhMOG/IFA was significantly reduced.

The translational relevance of the current study for the MS patient lies in the observation that it is apparently possible to modify the robust pathogen-trained immune system of adult marmosets via food,

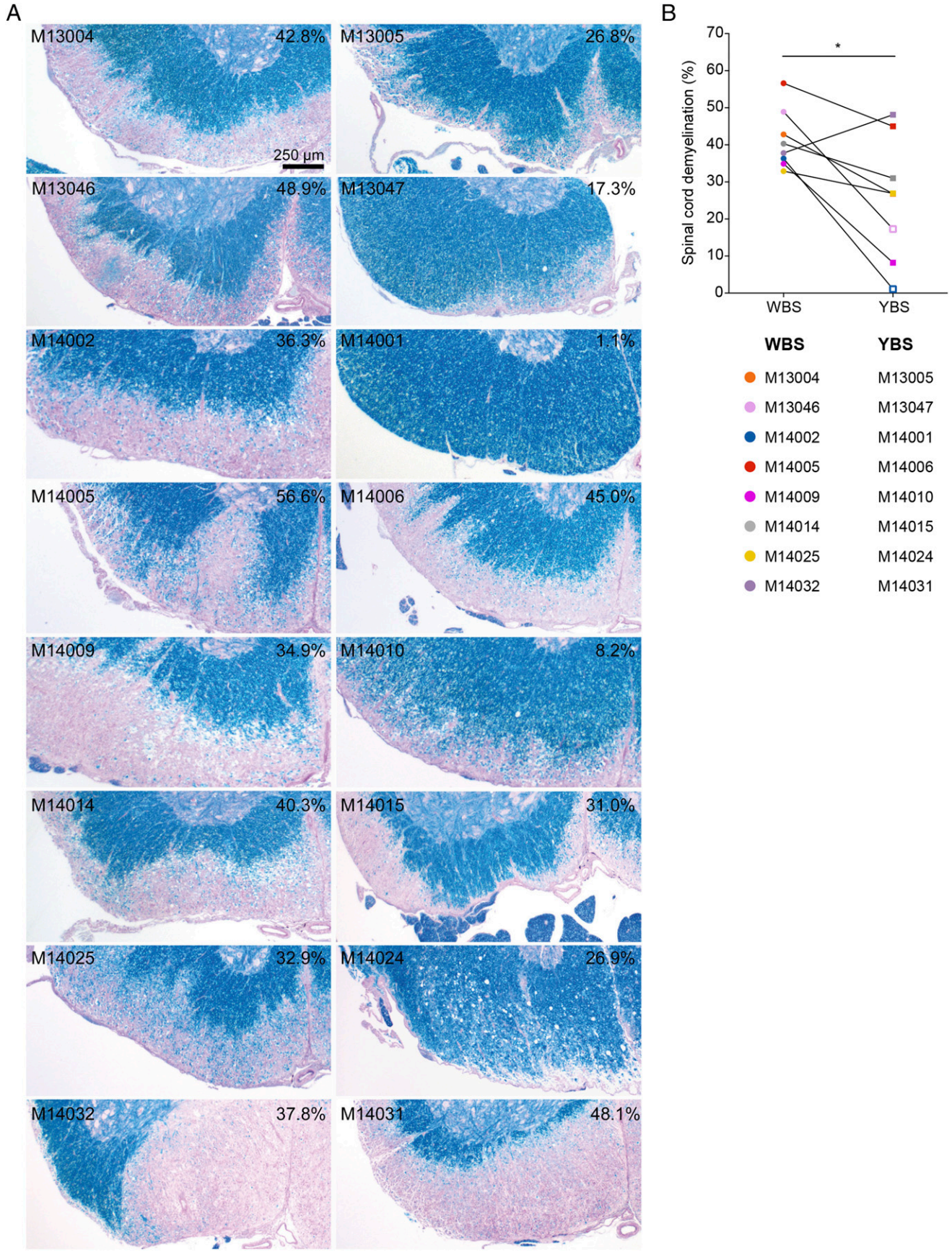

FIGURE 2. Reduced demyelination in the spinal cord of monkeys fed with the YBS. (**A**) Spinal cord sections were stained with Luxol fast blue/periodic acid–Schiff to assess the percentage of demyelination. Of each animal (numbers are in the upper left corner), a representative image is shown. The percentage of demyelination as a fraction of total surface area is shown in the upper right corner. (**B**) Paired analysis of spinal cord demyelination. Asymptomatic monkeys are indicated by an open square. *$p < 0.05$, t test.

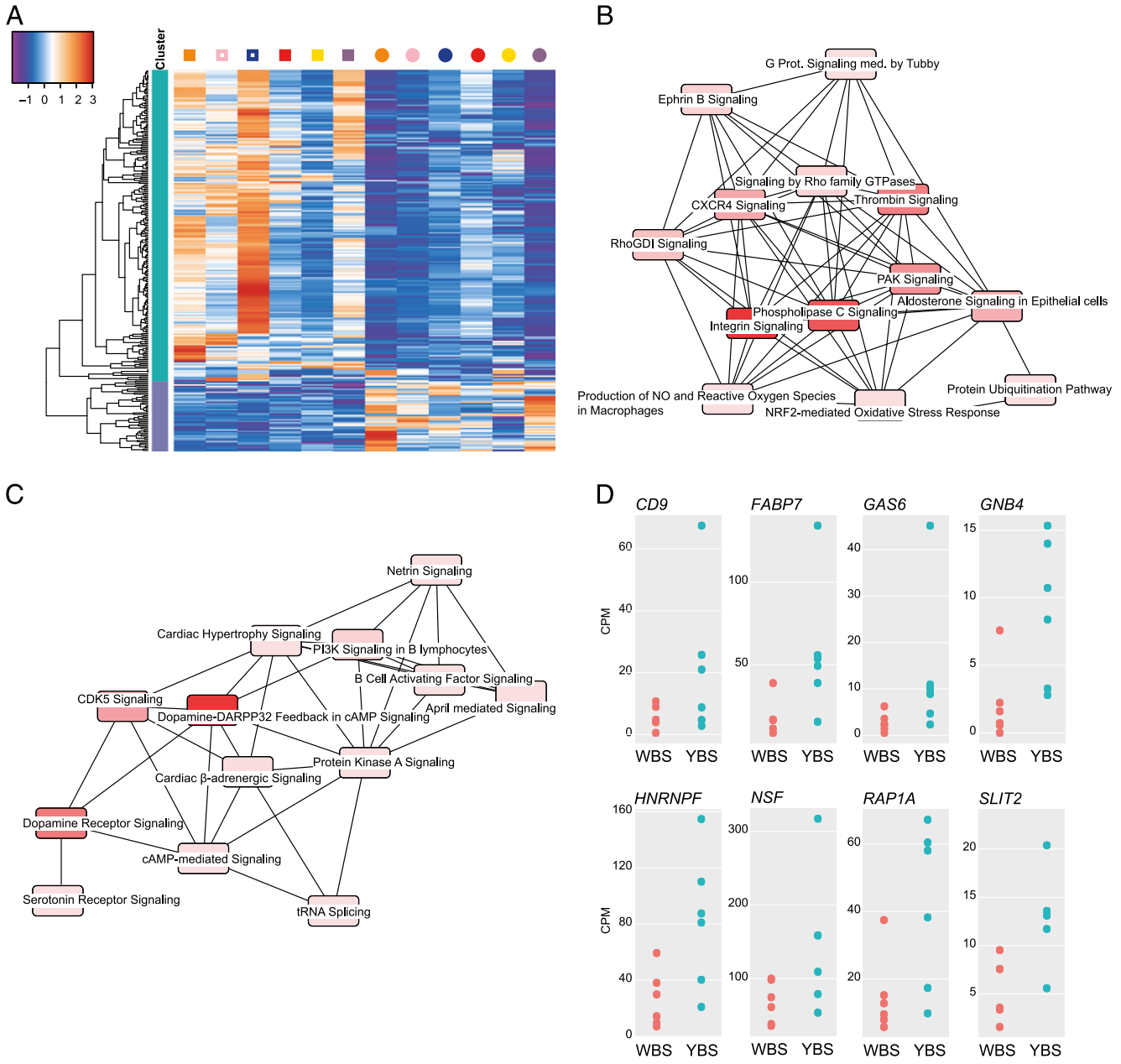

FIGURE 3. The CNS of monkeys fed with the YBS show signs of reduced apoptosis. (**A**) Heatmap displaying all genes differentially expressed (LogFC >1 and $p < 0.01$) between YBS and WBS. The YBS and WBS symbols correspond to monkey symbols in other figures. (**B** and **C**) IPA depicting the significant pathways associated with genes enriched in YBS (B) or WBS (C). Brighter red indicates higher significance as determined by IPA. (**D**) RNA expression levels of genes related to myelin biology in individual monkeys in counts per million (CPM). All depicted genes are differentially expressed between YBS and WBS.

resulting in reduced susceptibility to autoimmune neuroinflammatory disease. The work reported in this publication comprises an in-depth analysis of the effects of the dietary modification on (immuno) pathogenic processes relevant for EAE development in this model. The reported results show that the dietary modification exerts effects in different compartments along the gut–brain axis, namely: 1) the gut (i.e., microbiota composition), 2) the immune system (i.e., expression of CalHV3 as well as profiles and function of immune cells), and 3) the CNS (i.e., spinal cord demyelination and the brain transcriptome profile). It is important to emphasize in this study that the current study was not designed to identify which dietary compounds either individually or jointly drove differential immunity.

With respect to the effect of the dietary change on clinical signs, we observed that in the YBS-fed group two monkeys remained free of clinical signs, whereas their WBS-fed fraternal siblings developed full-blown clinical EAE. We did not expect a uniform effect, as the genetic and immunological heterogeneity in this highly refined outbred marmoset EAE model precludes a uniform response to an experimental variable. This was also observed in the response against a therapeutic mAb (44).

At the start of the study, the marmoset's gut microbiota was dominated by Actinobacteria, mainly represented by Bifidobacteria. Some of these strains have been isolated from marmoset feces before by other techniques (45). Bifidobacteria are needed for the metabolism of mono- and oligosaccharides and the digestion of complex carbohydrates (46). This group of bacteria is common in human neonates, in which they are required to digest milk (47, 48). In marmosets, Bifidobacteria facilitate the fermentation of the long-chain carbohydrates in gum, which is a

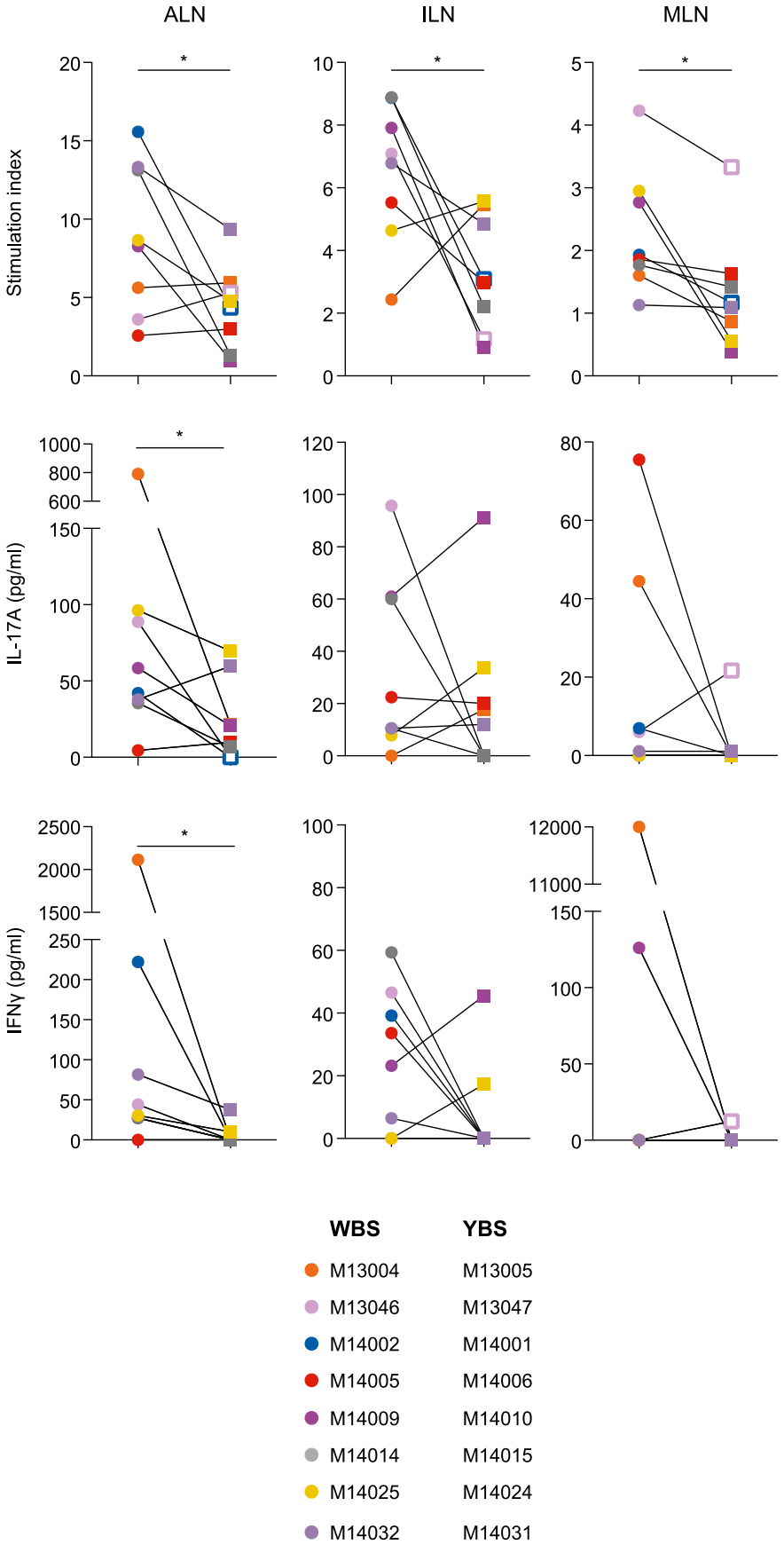

FIGURE 4. Dietary modification alters MOG-induced proliferation and cytokine production. Upper row, rhMOG-induced proliferation assayed by [^{3}H]thymidine incorporation expressed as stimulation index relative to nonstimulated cultures. Middle and bottom row, cytokine levels in culture supernatants collected after 48 h stimulation. Data are shown for individual marmosets with bottom left column (dots) the WBS monkeys; in the bottom right column are their siblings of the YBS monkeys (squares). Asymptomatic monkeys are indicated by an open square. *$p < 0.05$, t test.

main factor in their diet in the wild and in captivity. The high percentage of Actinobacteria contrasts with a recent paper in which marmoset gut microbiota were found to be dominated by Proteobacteria and Firmicutes (49). The differences may be explained by different food or technical differences, as we could confirm the high percentage of Bifidobacteria by FISH. The high

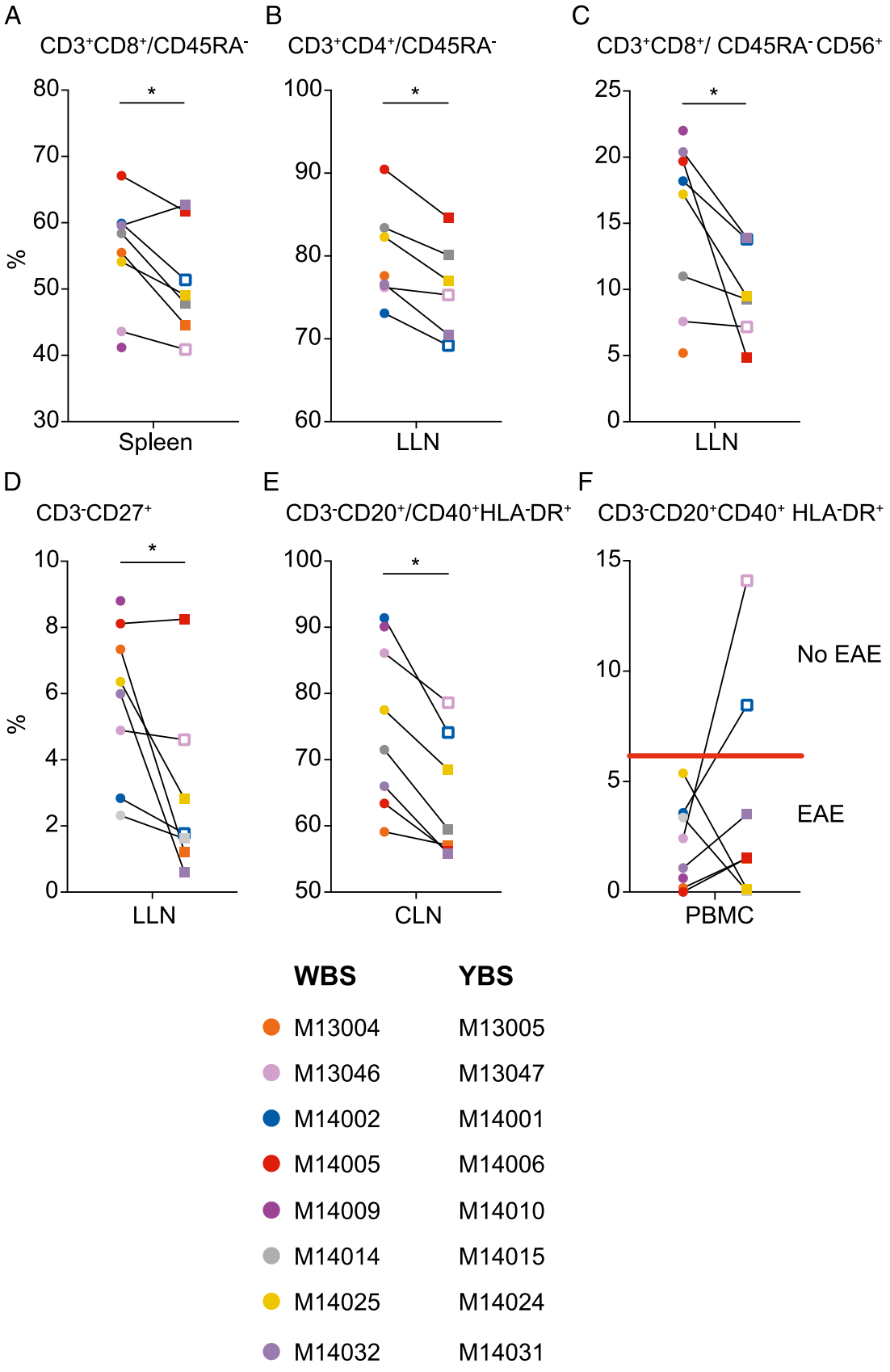

FIGURE 5. Cellular immune response changes within spinal cord–draining lymph nodes. MNC subsets were phenotyped with a broad panel of markers (**A**–**F**). Asymptomatic monkeys are indicated by an open square. *$p < 0.05$, *t* test.

abundance of Bifidobacteria at the start of the study may have been caused by the yogurt intake, as after feeding the WBS for 15 wk this percentage was profoundly reduced.

It is striking, however, that a detectable difference between the differently fed twin siblings was observed as late as 11 wk after the diet change and 3 wk after immunization, coinciding with first

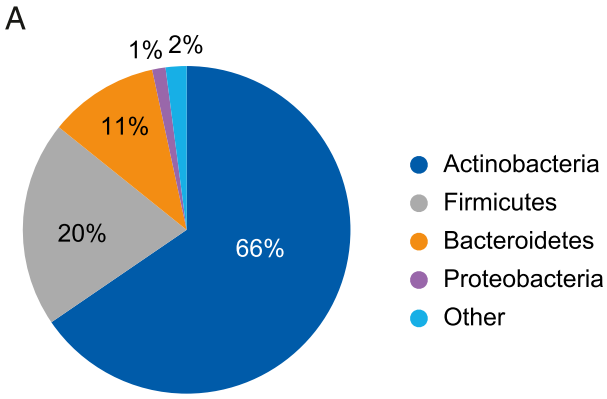

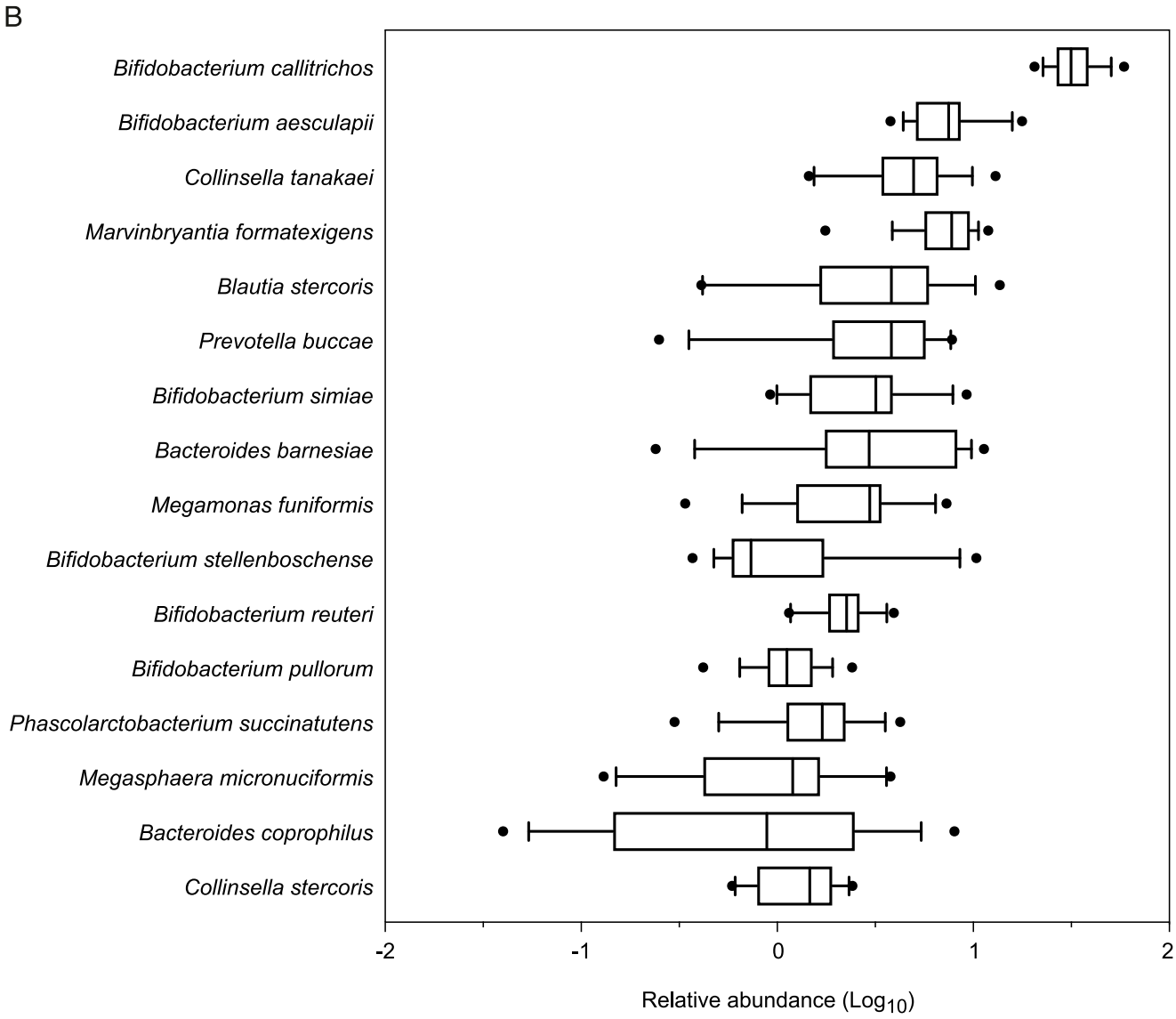

FIGURE 6. Marmoset microbiota composition is dominated by Bifidobacteria. (**A**) Frequencies of the most prevalent phyla in marmosets at day −56 and −7 (i.e., prior to immunization). (**B**) Box plot of the median relative abundance and variance of the most dominant species.

detectable Ab responses against rhMOG and linear encephalitogenic epitopes (see Supplemental Fig. 2). This may suggest that the diet change in itself was not sufficient for altering the microbiota composition and that the interplay between the diet and the immune responses against MOG may have affected microbiota composition.

The observed reduced CalHV3 expression in the immune compartment is important, as CalHV3-infected B cells have a key pathogenic role in the marmoset EAE model (15, 50). The mechanism underlying this CalHV3 reduction is not known, but there are potential leads from EBV. The lytic reactivation of EBV is controlled by medium- and short-chain fatty acids, which are

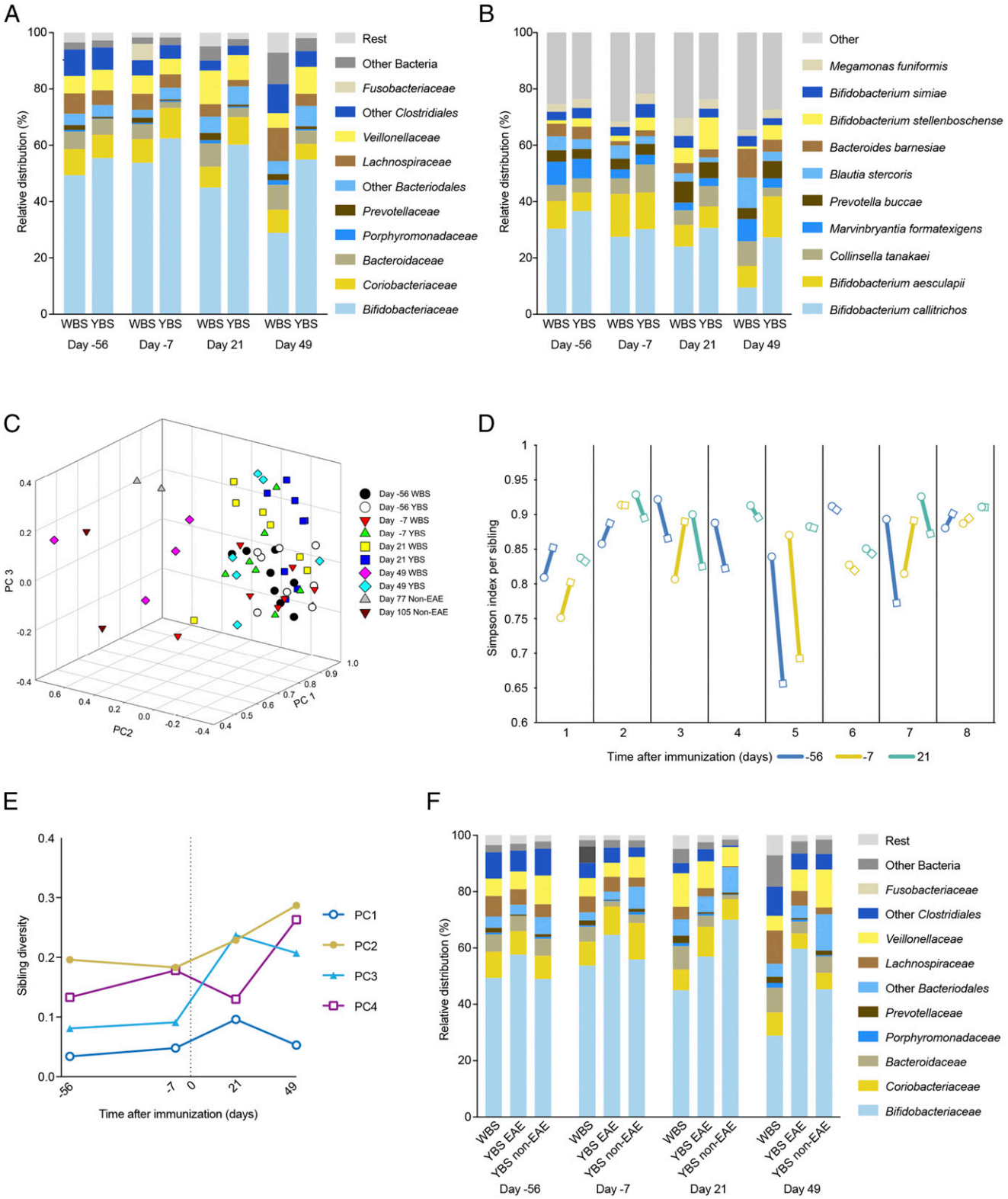

FIGURE 7. Diet influences on gut microbiota composition become evident after EAE induction. Shown is the relative distribution of the most abundant bacterial families (**A**) and species (**B**) analyzed before and after EAE induction. (**C**) Three-dimensional graph of PC1, 2, and 3. Each colored symbol represents the monkeys of one group and one time-point. PC1: describes 79% of variance, positive correlation with *Bifidobacterium callitrichos*; PC2: describes 6.8% of variance, positive correlation with the Simpson diversity, *Collinsella tanakei*, *M. formatexigens*, *Bacteroides barnesiae*, *Blautia stercoris*; negative correlation with *Bifidobacterium callitrichos*, *Bifidobacterium stellenboschense*, *Bifidobacterium simiae*; PC3: describes 3.5% of variance, positive correlation with Simpson diversity, *P. buccae*; negative correlation with *Bifidobacterium aesculapi*, *M. formatexigens*, *Bifidobacterium callitrichos*, *Blautia stercoris*; PC4: describes 3.2% of variance, positive correlation with *Bifidobacterium aesculapi*, *Bifidobacterium stellenboschense*; negative correlation with *M. formatexigens, Bacterioides barnesiae*, *Blautia stercoris.* (**D**) Simpson diversity index between siblings for day −56, −7, and 21. Twins are indicated on the *x*-axis; the YBS monkeys of twin 2 and 3 were asymptomatic. The open circles are the WBS monkeys, and the open squares are the YBS monkeys. (**E**) The difference (Δ) in PC values between siblings for PC1–4. (**F**) Relative distribution of the most abundant bacterial families with a distinction between the symptomatic (EAE) and asymptomatic (non-EAE) monkeys in the YBS group.

fermentation products of dietary fibers; butyrate stimulates and valproic acid suppresses EBV reactivation in vitro (51).

The whole-brain transcriptome profiling shows two profound effects of the dietary modification. First, the expression of genes implicated in myelination is increased in YBS-fed siblings. Second, genes associated with apoptosis show a reduced expression in YBS-fed siblings. In line with these findings, we observed reduced spinal cord pathology in the YBS-fed twin siblings coinciding with moderate albeit potentially meaningful changes in the spinal cord–draining LLN, namely a reduced percentage of memory $CD8^+$ T cells expressing CD56 and a reduced percentage of $CD3^-$ cells expressing CD27, suggestive of memory B cells. Previous work showed that $CD3^+CD8^+CD56^+$ T cells have a key pathogenic role in the EAE model induced with MOG34–56/IFA (52). Furthermore, both in mouse and marmoset EAE models, B cells contributing to EAE pathogenesis can be found in the subset with an Ag-experienced phenotype (19, 53). Also, in the lymph nodes that drain the immunization sites, a reduced T cell response to MOG was observed in the YBS group, suggesting that under the influence of the YBS the encephalitogenic immune response is mitigated.

Finally, the question remains by which factors development of clinical symptoms in two out of eight marmosets in the YBS-fed group were suppressed. At the start of the study, their microbiota composition was comparable to the other monkeys, but they started to deviate from the other monkeys in the YBS group after immunization. The day 21 and 49 fecal samples from these non-EAE monkeys contained high percentages of *P. buccae* and *Bifidobacterium stellenboschense*. Over time, microbiota changes became even more evident, which is remarkable, as these two monkeys had been fed the YBS since weaning. This observation suggests that the gut microbiota changes were at least in part related to the immunization. However, MOG-induced T cell responses and humoral responses in these monkeys did not markedly differ from the other monkeys in the YBS group. A noticeable difference, however, is the higher percentage of activated ($CD40^+$) B cells in the circulation of the two asymptomatic monkeys compared with the other monkeys in the YBS diet group that did develop clinically evident EAE. Previous studies showed that depletion of CD40-expressing B cells alleviated marmoset EAE (54), but it is well possible that the asymptomatic monkeys did not develop EAE because these B cells remained in the circulation rather than infiltrating the CNS.

In conclusion, to our knowledge, this is the first documented experimental evidence that the response of a pathogen-educated immune system of adult primates to a challenge with autoantigen can be modified via the food. The findings of this study position the established disease models in the marmoset monkey, such as those for autoimmune-mediated inflammatory and neurodegenerative disorders, as relevant platforms for translational studies into the interaction of gut microbiota, EBV-like herpesvirus, and pathogenic factors. Further research should reveal which dietary components individually or in concert are responsible for the distinct modifications of the pathological process.

Acknowledgments

We thank F. van Hassel for figure preparation, N. Brouwer, E. Wesseling, and R. Tonk (University Medical Center Groningen) for technical assistance, Dr. E. Remarque (Biomedical Primate Research Centre) for statistical analysis, and Prof. E. Steyerberg (Leiden University Medical Center, Leiden, the Netherlands) for methodological advice.

Disclosures

The authors have no financial conflicts of interest.

References

1. Dendrou, C. A., L. Fugger, and M. A. Friese. 2015. Immunopathology of multiple sclerosis. *Nat. Rev. Immunol.* 15: 545–558.
2. Ascherio, A., and K. L. Munger. 2015. EBV and autoimmunity. *Curr. Top. Microbiol. Immunol.* 390: 365–385.
3. Ascherio, A., and K. L. Munger. 2007. Environmental risk factors for multiple sclerosis. Part I: the role of infection. *Ann. Neurol.* 61: 288–299.
4. Belbasis, L., V. Bellou, E. Evangelou, J. P. Ioannidis, and I. Tzoulaki. 2015. Environmental risk factors and multiple sclerosis: an umbrella review of systematic reviews and meta-analyses. *Lancet Neurol.* 14: 263–273.
5. Blaser, M. J. 2017. The theory of disappearing microbiota and the epidemics of chronic diseases. *Nat. Rev. Immunol.* 17: 461–463.
6. Miyake, S., S. Kim, W. Suda, K. Oshima, M. Nakamura, T. Matsuoka, N. Chihara, A. Tomita, W. Sato, S. W. Kim, et al. 2015. Dysbiosis in the gut microbiota of patients with multiple sclerosis, with a striking depletion of species belonging to Clostridia XIVa and IV clusters. *PLoS One* 10: e0137429.
7. Jangi, S., R. Gandhi, L. M. Cox, N. Li, F. von Glehn, R. Yan, B. Patel, M. A. Mazzola, S. Liu, B. L. Glanz, et al. 2016. Alterations of the human gut microbiome in multiple sclerosis. *Nat. Commun.* 7: 12015.
8. Chen, J., N. Chia, K. R. Kalari, J. Z. Yao, M. Novotna, M. M. Paz Soldan, D. H. Luckey, E. V. Marietta, P. R. Jeraldo, X. Chen, et al. 2016. Multiple sclerosis patients have a distinct gut microbiota compared to healthy controls. *Sci. Rep.* 6: 28484.
9. Berer, K., L. A. Gerdes, E. Cekanaviciute, X. Jia, L. Xiao, Z. Xia, C. Liu, L. Klotz, U. Stauffer, S. E. Baranzini, et al. 2017. Gut microbiota from multiple sclerosis patients enables spontaneous autoimmune encephalomyelitis in mice. *Proc. Natl. Acad. Sci. USA* 114: 10719–10724.
10. Cekanaviciute, E., B. B. Yoo, T. F. Runia, J. W. Debelius, S. Singh, C. A. Nelson, R. Kanner, Y. Bencosme, Y. K. Lee, S. L. Hauser, et al. 2017. Gut bacteria from multiple sclerosis patients modulate human T cells and exacerbate symptoms in mouse models. [Published erratum appears in 2017 *Proc. Natl. Acad. Sci. USA* 114: E8943.] *Proc. Natl. Acad. Sci. USA* 114: 10713–10718.
11. Berer, K., M. Mues, M. Koutrolos, Z. A. Rasbi, M. Boziki, C. Johner, H. Wekerle, and G. Krishnamoorthy. 2011. Commensal microbiota and myelin autoantigen cooperate to trigger autoimmune demyelination. *Nature* 479: 538–541.
12. 't Hart, B. A., B. Gran, and R. Weissert. 2011. EAE: imperfect but useful models of multiple sclerosis. *Trends Mol. Med.* 17: 119–125.
13. 't Hart, B. A., Y. van Kooyk, J. J. Geurts, and B. Gran. 2015. The primate autoimmune encephalomyelitis model; a bridge between mouse and man. *Ann. Clin. Transl. Neurol.* 2: 581–593.
14. Vanheusden, M., P. Stinissen, B. A. 't Hart, and N. Hellings. 2015. Cytomegalovirus: a culprit or protector in multiple sclerosis? *Trends Mol. Med.* 21: 16–23.
15. 'tHart, B. A., Y. S. Kap, E. Morandi, J. D. Laman, and B. Gran. 2016. EBV infection and multiple sclerosis: lessons from a marmoset model. *Trends Mol. Med.* 22: 1012–1024.
16. 't Hart, B. A., J. Dunham, B. W. Faber, J. D. Laman, J. van Horssen, J. Bauer, and Y. S. Kap. 2017. A B cell-driven autoimmune pathway leading to pathological hallmarks of progressive multiple sclerosis in the marmoset experimental autoimmune encephalomyelitis model. *Front. Immunol.* 8: 804.
17. Kerlero de Rosbo, N., M. Hoffman, I. Mendel, I. Yust, J. Kaye, R. Bakimer, S. Flechter, O. Abramsky, R. Milo, A. Karni, and A. Ben-Nun. 1997. Predominance of the autoimmune response to myelin oligodendrocyte glycoprotein (MOG) in multiple sclerosis: reactivity to the extracellular domain of MOG is directed against three main regions. *Eur. J. Immunol.* 27: 3059–3069.
18. Jagessar, S. A., M. Vierboom, E. L. Blezer, J. Bauer, B. A. Hart, and Y. S. Kap. 2013. Overview of models, methods, and reagents developed for translational autoimmunity research in the common marmoset (Callithrix jacchus). *Exp. Anim.* 62: 159–171.
19. Anwar Jagessar, S., Z. Fagrouch, N. Heijmans, J. Bauer, J. D. Laman, L. Oh, T. Migone, E. J. Verschoor, and B. A. 't Hart. 2013. The different clinical effects of anti-BLyS, anti-APRIL and anti-CD20 antibodies point at a critical pathogenic role of γ-herpesvirus infected B cells in the marmoset EAE model. *J. Neuroimmune Pharmacol.* 8: 727–738.
20. Kim, D., B. Langmead, and S. L. Salzberg. 2015. HISAT: a fast spliced aligner with low memory requirements. *Nat. Methods* 12: 357–360.
21. Li, H., B. Handsaker, A. Wysoker, T. Fennell, J. Ruan, N. Homer, G. Marth, G. Abecasis, and R. Durbin, 1000 Genome Project Data Processing Subgroup. 2009. The sequence alignment/map format and SAMtools. *Bioinformatics* 25: 2078–2079.
22. Anders, S., P. T. Pyl, and W. Huber. 2015. HTSeq--a Python framework to work with high-throughput sequencing data. *Bioinformatics* 31: 166–169.
23. George, N. I., and C. W. Chang. 2014. DAFS: a data-adaptive flag method for RNA-sequencing data to differentiate genes with low and high expression. *BMC Bioinformatics* 15: 92.
24. He, T., M. G. Priebe, Y. Zhong, C. Huang, H. J. Harmsen, G. C. Raangs, J. M. Antoine, G. W. Welling, and R. J. Vonk. 2008. Effects of yogurt and bifidobacteria supplementation on the colonic microbiota in lactose-intolerant subjects. *J. Appl. Microbiol.* 104: 595–604.
25. Harmsen, H. J., G. C. Raangs, T. He, J. E. Degener, and G. W. Welling. 2002. Extensive set of 16S rRNA-based probes for detection of bacteria in human feces. *Appl. Environ. Microbiol.* 68: 2982–2990.
26. Yu, Z., and M. Morrison. 2004. Improved extraction of PCR-quality community DNA from digesta and fecal samples. *Biotechniques* 36: 808–812.
27. van Praagh, J. B., M. C. de Goffau, I. S. Bakker, H. J. Harmsen, P. Olinga, and K. Havenga. 2016. Intestinal microbiota and anastomotic leakage of stapled colorectal anastomoses: a pilot study. *Surg. Endosc.* 30: 2259–2265.

28. Bartram, A. K., M. D. Lynch, J. C. Stearns, G. Moreno-Hagelsieb, and J. D. Neufeld. 2011. Generation of multimillion-sequence 16S rRNA gene libraries from complex microbial communities by assembling paired-end illumina reads. *Appl. Environ. Microbiol.* 77: 3846–3852.
29. Werner, J. J., D. Zhou, J. G. Caporaso, R. Knight, and L. T. Angenent. 2012. Comparison of Illumina paired-end and single-direction sequencing for microbial 16S rRNA gene amplicon surveys. *ISME J.* 6: 1273–1276.
30. Masella, A. P., A. K. Bartram, J. M. Truszkowski, D. G. Brown, and J. D. Neufeld. 2012. PANDAseq: paired-end assembler for illumina sequences. *BMC Bioinformatics* 13: 31.
31. Ludwig, W., O. Strunk, R. Westram, L. Richter, H. Meier, A. Yadhukumar,, T. Buchner,, S. Lai,, G. Steppi,, Jobb,et al. 2004. ARB: a software environment for sequence data. *Nucleic Acids Res.* 32: 1363–1371.
32. Shimwell, M., B. F. Warrington, and J. S. Fowler. 1979. Dietary habits relating to 'wasting marmoset syndrome' (WMS). *Lab. Anim.* 13: 139–142.
33. Gacad, M. A., and J. S. Adams. 1991. Endogenous blockade of 1,25-dihydroxyvitamin D-receptor binding in New World primate cells. *J. Clin. Invest.* 87: 996–1001.
34. Kap, Y. S., N. van Driel, E. Blezer, P. W. Parren, W. K. Bleeker, J. D. Laman, J. L. Craigen, and B. A. 't Hart. 2010. Late B cell depletion with a human anti-human CD20 IgG1κ monoclonal antibody halts the development of experimental autoimmune encephalomyelitis in marmosets. *J. Immunol.* 185: 3990–4003.
35. Kap, Y. S., N. van Driel, J. D. Laman, P. P. Tak, and B. A. 't Hart. 2014. CD20+ B cell depletion alters T cell homing. *J. Immunol.* 192: 4242–4253.
36. Jagessar, S. A., I. R. Holtman, S. Hofman, E. Morandi, N. Heijmans, J. D. Laman, B. Gran, B. W. Faber, S. I. van Kasteren, B. J. Eggen, and B. A. 't Hart. 2016. Lymphocryptovirus infection of nonhuman primate B cells converts destructive into productive processing of the pathogenic CD8 T cell epitope in myelin oligodendrocyte glycoprotein. *J. Immunol.* 197: 1074–1088.
37. Kap, Y. S., P. Smith, S. A. Jagessar, E. Remarque, E. Blezer, G. J. Strijkers, J. D. Laman, R. Q. Hintzen, J. Bauer, H. P. Brok, and B. A. 't Hart. 2008. Fast progression of recombinant human myelin/oligodendrocyte glycoprotein (MOG)-induced experimental autoimmune encephalomyelitis in marmosets is associated with the activation of MOG34-56-specific cytotoxic T cells. *J. Immunol.* 180: 1326–1337.
38. Jagessar, S. A., N. Heijmans, E. L. Blezer, J. Bauer, J. H. Blokhuis, J. A. Wubben, J. W. Drijfhout, P. J. van den Elsen, J. D. Laman, and B. A. Hart. 2012. Unravelling the T-cell-mediated autoimmune attack on CNS myelin in a new primate EAE model induced with MOG34-56 peptide in incomplete adjuvant. *Eur. J. Immunol.* 42: 217–227.
39. Olsson, T., L. F. Barcellos, and L. Alfredsson. 2017. Interactions between genetic, lifestyle and environmental risk factors for multiple sclerosis. *Nat. Rev. Neurol.* 13: 25–36.
40. van den Hoogen, W. J., J. D. Laman, and B. A. 't Hart. 2017. Modulation of multiple sclerosis and its animal model experimental autoimmune encephalomyelitis by food and gut microbiota. *Front. Immunol.* 8: 1081.
41. Colpitts, S. L., E. J. Kasper, A. Keever, C. Liljenberg, T. Kirby, K. Magori, L. H. Kasper, and J. Ochoa-Repáraz. 2017. A bidirectional association between the gut microbiota and CNS disease in a biphasic murine model of multiple sclerosis. *Gut Microbes* 8: 561–573.
42. Petta, I., J. Fraussen, V. Somers, and M. Kleinewietfeld. 2018. Interrelation of diet, gut microbiome, and autoantibody production. *Front. Immunol.* 9: 439.
43. Jagessar, S. A., N. Heijmans, E. L. Blezer, J. Bauer, R. Weissert, and B. A. 't Hart. 2015. Immune profile of an atypical EAE model in marmoset monkeys immunized with recombinant human myelin oligodendrocyte glycoprotein in incomplete Freund's adjuvant. *J. Neuroinflammation* 12: 169.
44. Dunham, J., L. F. Lee, N. van Driel, J. D. Laman, I. Ni, W. Zhai, G. H. Tu, J. C. Lin, J. Bauer, B. A. 't Hart, and Y. S. Kap. 2016. Blockade of CD127 exerts a dichotomous clinical effect in marmoset experimental autoimmune encephalomyelitis. *J. Neuroimmune Pharmacol.* 11: 73–83.
45. Endo, A., Y. Futagawa-Endo, P. Schumann, R. Pukall, and L. M. Dicks. 2012. Bifidobacterium reuteri sp. nov., Bifidobacterium callitrichos sp. nov., Bifidobacterium saguini sp. nov., Bifidobacterium stellenboschense sp. nov. and Bifidobacterium biavatii sp. nov. isolated from faeces of common marmoset (Callithrix jacchus) and red-handed tamarin (Saguinus midas). *Syst. Appl. Microbiol.* 35: 92–97.
46. Turroni, F., D. van Sinderen, and M. Ventura. 2011. Genomics and ecological overview of the genus Bifidobacterium. *Int. J. Food Microbiol.* 149: 37–44.
47. Favier, C. F., E. E. Vaughan, W. M. De Vos, and A. D. Akkermans. 2002. Molecular monitoring of succession of bacterial communities in human neonates. *Appl. Environ. Microbiol.* 68: 219–226.
48. Palmer, C., E. M. Bik, D. B. DiGiulio, D. A. Relman, and P. O. Brown. 2007. Development of the human infant intestinal microbiota. *PLoS Biol.* 5: e177.
49. Albert, K., A. Rani, and D. A. Sela. 2018. The comparative genomics of Bifidobacterium callitrichos reflects dietary carbohydrate utilization within the common marmoset gut. *Microb. Genom.* DOI: 10.1099/mgen.0.000183.
50. 't Hart, B. A., S. A. Jagessar, K. Haanstra, E. Verschoor, J. D. Laman, and Y. S. Kap. 2013. The primate EAE model points at EBV-infected B cells as a preferential therapy target in multiple sclerosis. *Front. Immunol.* 4: 145.
51. Gorres, K. L., D. Daigle, S. Mohanram, and G. Miller. 2014. Activation and repression of Epstein-Barr Virus and Kaposi's sarcoma-associated herpesvirus lytic cycles by short- and medium-chain fatty acids. *J. Virol.* 88: 8028–8044.
52. Jagessar, S. A., Y. S. Kap, N. Heijmans, N. van Driel, L. van Straalen, J. J. Bajramovic, H. P. M. Brok, E. L. A. Blezer, J. Bauer, J. D. Laman, and B. A. 't Hart. 2010. Induction of progressive demyelinating autoimmune encephalomyelitis in common marmoset monkeys using MOG34-56 peptide in incomplete freund adjuvant. *J. Neuropathol. Exp. Neurol.* 69: 372–385.
53. Baker, D., M. Marta, G. Pryce, G. Giovannoni, and K. Schmierer. 2017. Memory B cells are major targets for effective immunotherapy in relapsing multiple sclerosis. *EBioMedicine* 16: 41–50.
54. Jagessar, S. A., N. Heijmans, J. Bauer, E. L. Blezer, J. D. Laman, N. Hellings, and B. A. 't Hart. 2012. B-cell depletion abrogates T cell-mediated demyelination in an antibody-nondependent common marmoset experimental autoimmune encephalomyelitis model. *J. Neuropathol. Exp. Neurol.* 71: 716–728.